

## Conference Paper

# Current Control Optimization for Grid-tied Inverters Using Cuckoo Search Algorithm

João Faria, José Pombo, Maria do Rosário Calado, and Sílvio Mariano

Universidade da Beira Interior

## Abstract

One of the most decisive factors for a smooth and stable operation of an DC / AC converter connected to the power grid are the gains used in the current controllers. This paper proposes the use of the Cuckoo Search optimization algorithm via Lévy Flights to facilitate the determination of the optimal gains of the grid connected DC / AC converters. With the proposed algorithm, it becomes possible to determine the optimal gains of the current controllers of the DC / AC converters connected with the grid thus improving their stability, accuracy and response time.

**Keywords:** DC/AC converters, Cuckoo search, Optimization, Current controllers

Corresponding Author:

João Faria

joao.pedro.faria@ubi.pt

Received: 26 November 2019

Accepted: 13 May 2020

Published: 2 June 2020

Publishing services provided by  
Knowledge E

© João Faria et al. This article is distributed under the terms of the [Creative Commons Attribution License](#), which permits unrestricted use and redistribution provided that the original author and source are credited.

Selection and Peer-review under the responsibility of the ICEUBI2019 Conference Committee.

## 1. Introduction

Currently, the planet suffers negative impacts due to the exploitation of its natural resources. However, in order to reduce the damage caused by humans, some alternative energy production processes have been set up to address much of the energy need. From this context, it can be said that renewable energy will be a great asset for the future. The use of this type of energy, obtained through the direct transformation of natural resources, is currently a great trend, not only because they are inexhaustible sources, but also because they have a reduced ecological footprint. At this moment, the most attractive solutions are photovoltaic or wind production. To enable the synchronization of this type of renewable production with the power grid, it is essential to use a DC-AC converter, commonly called as inverter. However, the control loops required for robust and effective control of this type of converter are extremely complex and has therefore been of great interest to the scientific community. Fig. 1 illustrates the main control loops that are transverse to any type of inverter interconnected with the power grid. These can be divided into four groups: in a first group, the MPPT control loops responsible for extracting maximum power from endogenous and renewable sources; a second group is the DC Link Control Scheme. The purpose of this voltage control loop is to control the bus voltage by ensuring the energy balance; in a third group, it can be considered

## OPEN ACCESS

the current control loops that ensure that the current injected into the mains follows the specified reference; lastly, the synchronization-associated control loops (PLL), which are responsible for extracting the voltage characteristics of the power grid. However, one of the biggest obstacles to the proper functioning of this type of control loop is the determination of the optimum gains for current controllers. It is therefore common in the literature to use optimization algorithms to aid their determination. This paper proposes the use of the Cuckoo Search optimization algorithm via Lévy Flights to facilitate the determination of the optimal gains of the grid connected inverters.

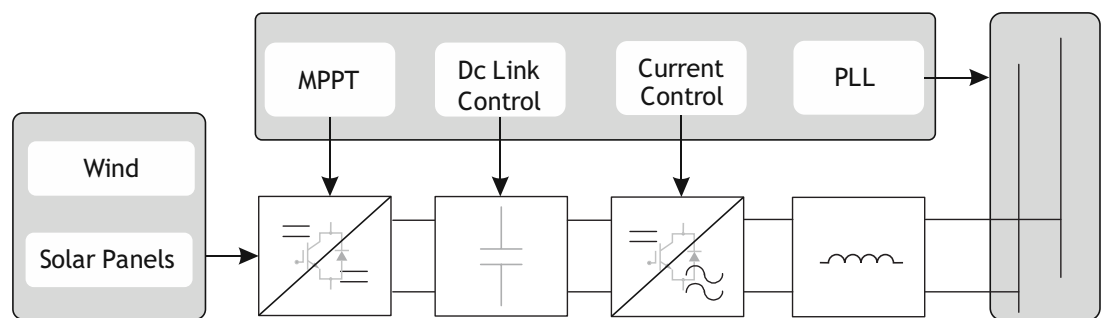


**Figure 1:** Control loops associated with an inverter connected to the power grid.

## 2. Current Controllers

### 2.1. Hysteresis Band Controllers

The hysteresis band controllers, outlined in Fig. 2, are widespread controllers in the literature because they are simple to implement, low cost and robust, acting from the instantaneous current value feedback [1]. These controllers can be used in both stationary and synchronous references, using Clark and Park transforms, respectively.

However, this type of controller has some disadvantages, such as the use of a variable switching frequency, which depends on the hysteresis band around the selected reference signal as well as the sampling period. Another disadvantage is that the resulting current waveform depends on the selected hysteresis band, a smaller band results in a higher switching frequency, leading to higher losses. In contrast, a larger band results in a lower switching frequency, lower losses, causing unwanted harmonic components to appear in the resulting current waveform. Another disadvantage lies in filter sizing as a consequence of using a variable switching frequency.

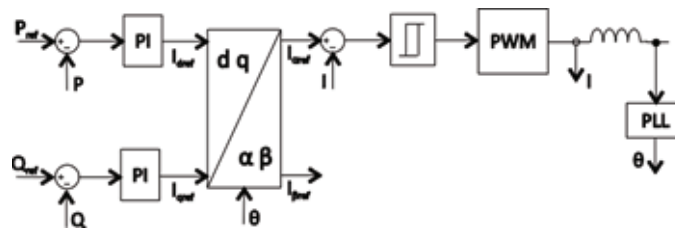


Figure 2: Block diagram of the hysteresis band current controller in the stationary axis.

### 2.2. Resonant Proportional Controllers (PR)

The resonant proportional controllers (PR) in the stationary reference is another current controller and a popular solution in the literature, as outlined in Fig. 3.

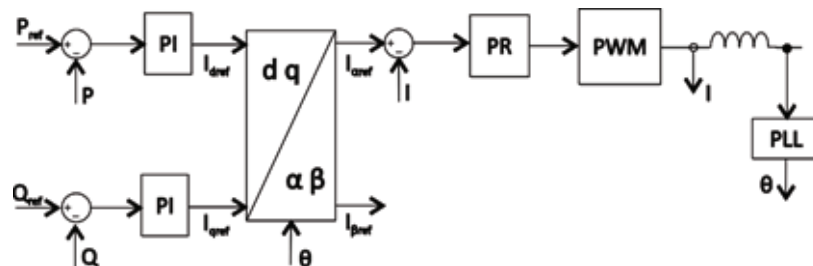


Figure 3: Block diagram of the PR current.

The main reason for using such controllers is the inability of classic PI controllers to follow a sinusoidal reference without stationary error. This is because the PI controller gain is inversely proportional to frequency, losing the ability to override the stationary error with increasing frequency [2], [3]. In contrast, PR controllers have a high gain in their resonant frequency and approximately zero out of it [4]. Another reason for using these controllers is the lower number of trigonometric calculations required.

The ideal transfer function of the PR controllers is expressed by equation (1), where  $w_n$  is the resonant frequency of the controller, and the constants  $K_p$  and  $K_i$  the proportional gain and the integral gain, respectively. The bandwidth around the resonant frequency depends on the value of the integral gain; a small value gives a very narrow band, while a large value in proportional gain will cause a larger band around the resonant frequency.

$$H(s) = K_p + K_i \frac{s}{s^2 - w_n^2} \tag{1}$$

### 2.3. Integral Proportional Controller (PI)

Another well documented solution in the literature, illustrated in Fig. 4, are the controllers in the synchronous reference frame and expressed by equation (2). The transformation

to synchronous reference has the advantage of presenting continuous variables over time, allowing the use of classic PID controllers [1], [5], [6].

$$H(s) = K_p + \frac{K_i}{s} \tag{2}$$

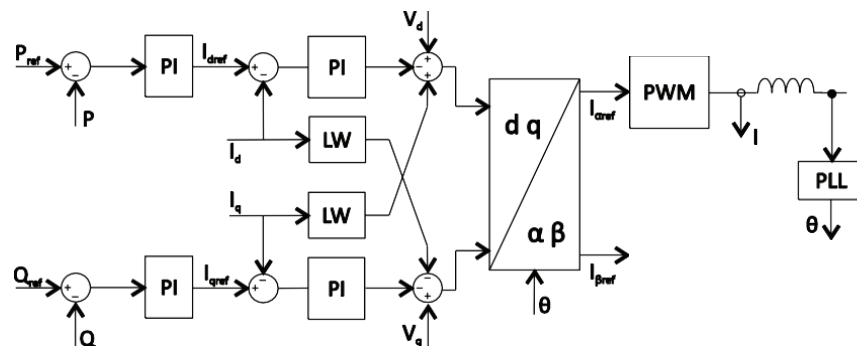


Figure 4: Block diagram of PI current controller in synchronous axis.

Other control strategies can be found in the literature, although less expressive when compared to the described strategies, such as sliding mode control, deadbeat control, repetitive control, fuzzy control [7].

### 3. Optimization Algorithm

#### 3.1. Cuckoo Search optimization algorithm via Lévy Flights.

The intrinsic idea of this algorithm is that each agent (cuckoo) randomly lays its egg on a fixed and predetermined number of host bird nests. However, if the host (host bird) discovers that the egg is not yours, he will leave his nest and build a new nest.

In the algorithm, this procedure (cuckoo egg to be discovered) is controlled by a probability  $p_a \in [0, 1]$  and the generation of new nests performed randomly through a local random walk, expressed by equation (3), [8].

$$x_i^{t+1} = x_i^t + \alpha s \otimes H(p_a - \varepsilon) \otimes (x_j^t - x_k^t) \tag{3}$$

Where  $x_j^t$  and  $x_k^t$  are two randomly selected nests,  $H$  represents a step function,  $\varepsilon$  a random number with a normal distribution,  $\otimes$  represents the multiplication between the values of the matrices and  $s$  the size of the step amplitude.

However, the algorithm combines a local random walk with a global random walk in which a fraction of the nests with worse aptitude are replaced according to a Lévy distribution, according to equation (4), [8]:

$$x_i^{t+1} = x_i^t + \alpha L(s, \lambda) \tag{4}$$

where,

$$L(s, \lambda) = \frac{\lambda \Gamma(\lambda) \sin\left(\frac{\pi\lambda}{2}\right)}{\pi} \frac{1}{s^{1+\lambda}} s \gg s_0 > 0 \quad (5)$$

and  $\alpha$  is the size of the step amplitude normally calculated by equation (6):

$$\alpha = 0.01s \otimes (x_i^t - x_{best}) \quad (6)$$

The Lévy distribution is a stable distribution of infinite variance, so it is commonly referred to as a long tail distribution. Using this type of distribution will cause some solutions to be generated close to the best solution so far. However, a portion is generated at random and distant locations of the best solution so far, ensuring greater exploration of the search space avoiding premature convergence.

One of the most efficient and simple ways to implement a symmetric Lévy distribution is based on the algorithm developed by [9], called the Mantegna algorithm. The size of the amplitude of step  $s$  can be calculated by equation (7):

$$s = \frac{u}{|v|^{\frac{1}{\beta}}} \quad (7)$$

where  $u$  and  $v$  represent a random value with a normal distribution where  $u \sim N(0, \sigma_u^2)$  and  $v \sim N(0, \sigma_v^2)$ , with

$$\sigma_u = \left\{ \frac{\Gamma(1 + \beta) \sin\left(\frac{\pi\beta}{2}\right)}{\Gamma\left(\frac{1+\beta}{2}\right) \beta 2^{\frac{\beta-1}{2}}} \right\}, \sigma_v = 1 \quad (8)$$

where  $\beta$  is a parameter comprised between [1, 2] and  $\Gamma$  represents a function *Gamma*. Algorithm 1 illustrates the pseudocode of the Cuckoo Search optimization algorithm applied to the problem of determining the optimal gains of current controllers.

## 4. Optimization

A photovoltaic system interconnected with the power grid was developed in a Matlab / Simulink simulation environment to optimize the gains of current controllers.

To optimize the gains of the PR controllers the system of Fig. 5 was created, composed of two PR controllers characterized by equation (1) thus allowing the control of active and reactive powers.

In order to optimize the PI controller gains on the synchronous axis, the system of Fig. 6 composed by two PI controllers characterized by equation (2) was implemented.

Both systems consists of a DC-AC converter with a Highly Efficient and Reliable Inverter Concept (HERIC) topology and a Hybrid SPWM with a switching frequency of

**Algorithm 1:** Current controller optimization algorithm.

```

Position the population of host nests;
Set the number of maximum iterations → iter_max;
While (iter < iter_max)
{
    Generate a random cuckoo by Lévy Flights;
    Calculate parameters dependent on  $K_P$  and  $K_R$ ;
    Simulate model;
    While (Time < Simulation Time)
    {
        };
    Calculate  $F_i$ ;
    Choose a nest  $j$  between  $n$  randomly;
    If  $F_i < F_j$ 
    {
        Replaces  $j$  with the new solution  $i$ ;
    }
    Sorts the nests and determines the best;
    for  $i=1:0.75n$ 
    {
        If  $\text{rand}(e) < p_a$ 
        {
            Generate new nest;
            Calculate parameters dependent on  $K_P$  and  $K_R$ ;
            Simulate model;
            While (Time < Simulation Time)
            {
                };
            Calculate  $F_i$ ;
        }
    }
}
    
```

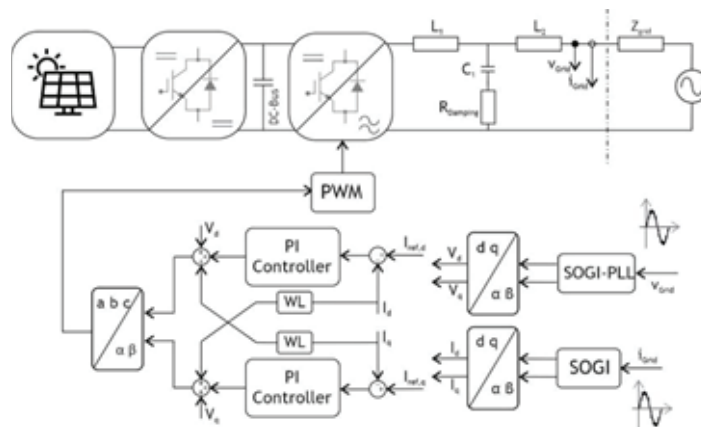


**Figure 5:** PI current controller structure.

20kHz. This topology uses two additional switches to ensure decoupling (AC decoupling) between the photovoltaic panels and the mains during freewheeling diode operation periods.

In both controllers the grid synchronization mechanism used was the Second Order Generalized Integrator Phase Locked Loop (SOGI-PLL) with a sampling frequency of 50kHz. The coupling with the electric network was performed through an LCL filter that allows an attenuation of 60 dB/dec. However, it has a disadvantage in introducing a resonant frequency into the system, causing distortion in the output current or causing

the system to lose stability. To mitigate this disadvantage, passive damping was used with the introduction of a series resistor.

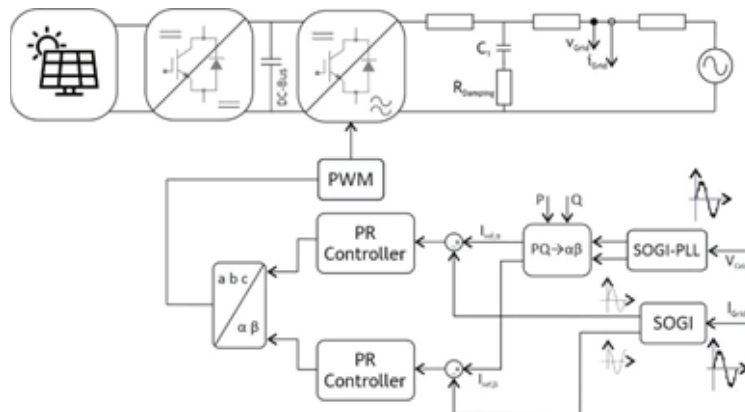


Figure 6: PR current controller structure.

To determine the optimal gains of the controllers described in Figs. 3 and 4, Algorithm 1 was applied, composed by a population of twenty host nests positioned linearly in the search space, and with a defined probability  $p_a$  of 0.25. Table 1 lists the search space limits for both drivers.

TABLE 1: Search Space Limits.

PR Controller				PI Controller			
$K_p$		$K_i$		$K_p$		$K_i$	
Lower Bound	Upper Bound	Lower Bound	Upper Bound	Lower Bound	Upper Bound	Lower Bound	Upper Bound
130000	200000	200	600	0.01	0.3	20	200

The objective function consists of the integral of time-weighted absolute error (ITAE) between the reference current and the output current represented by equation (8).

$$ITAE = \int_0^{\infty} t |I_{ref} - I_{out}| dt \tag{9}$$

## 5. PR Controllers

Figure 7 illustrates the evolution of current error in alpha and beta axes with optimized gains through the proposed algorithm and described in Table 2. From the analysis of that figure, it can be concluded that: i) the controllers have similar performances, but the alpha axis controller performs slightly better than the the beta axis controller; ii) after establishment time the error on the alpha axis is less than +/- 0.006 A; (iii) in the beta axis, the error after establishment time is less than +/- 0.015 A.

TABLE 2: Simulation results for optimization of PR controller gains

$K_{p1}$	$K_{p2}$	$K_{R1}$	$K_{R2}$	$F$
577.1601	577.1601	190764.96	190764.96	407.0287

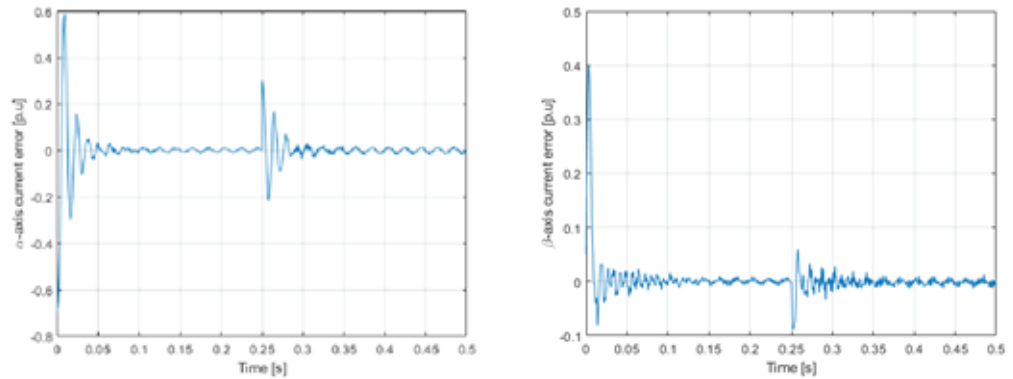


Figure 7: Evolution of current error in the Alpha and Beta axes.

Figure 8 shows the evolution of main voltage and the injected current at the coupling point where we can verify the excellent performance of the PR controller in both overshoot and setup time after a change in current reference from 0.7 p.u. to 1 p.u at a time greater than 0.25 s.

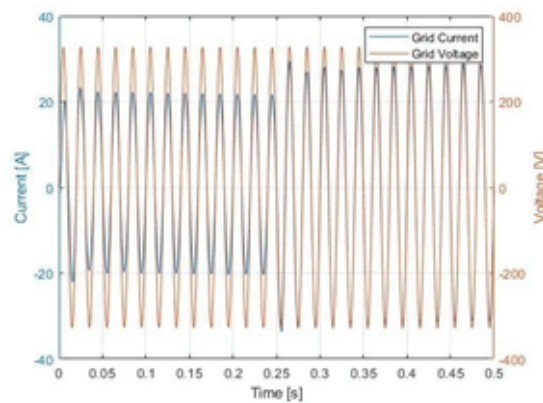


Figure 8: Evolution of the injected current and the grid voltage.

## 6. PI Controllers

Figure 9 illustrates the evolution of current error in direct and quadrature axes with the optimized gains obtained from the proposed algorithm with parameters described in Table 3.

From the analysis of that figure, it can be concluded that: i) the controller has an establishment time close to 0.06 s, having similar performance to the PR controller; ii)

after set-up, the controller has an error of +/- 0.006 A showing similar performance to the PR controller; iii) the controller exhibits worse performance at startup when compared to the PR controller.

TABLE 3: Simulation results for PI controller gain optimization

$K_{p1}$	$K_{p2}$	$K_{I1}$	$K_{I2}$	$F$
0.0476	0.0476	38.6004	38.6004	383.4022

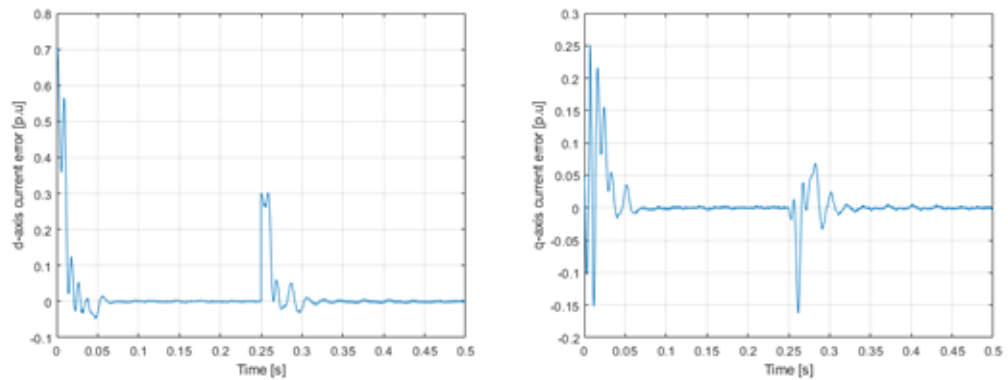


Figure 9: Evolution of current error in d and q axes.

Fig. (10) shows the evolution of mains voltage and injected current at the coupling point where we can verify the excellent performance of the PI controller.

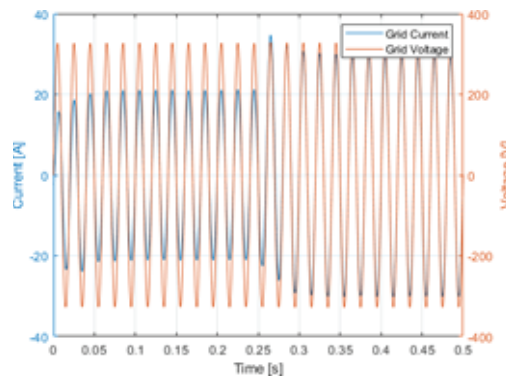


Figure 10: Evolution of the injected current and the grid voltage.

## 7. Conclusions

In this paper, it was proposed the use of the Cuckoo Search algorithm to optimize the gain of current controllers for grid connected inverters. The proposed optimization method allows to easily determine the optimum gains for current controllers of inverters interconnected with the grid. Simulation results show that the proposed optimization algorithm can easily determine the optimal gains for the PR and PI current controllers.

With the proposed algorithm, it becomes possible to optimize the gains of the current controllers of the DC / AC converters interconnected with the power grid thus improving their stability, accuracy and response time.

## Acknowledgements

This work is funded by FCT/MEC through national funds and when applicable co-funded by FEDER–PT2020 partnership agreement under the project UID/EEA/50008/2019.

## References

- [1] M. Monfared and S. Golestan, "Control strategies for single-phase grid integration of small-scale renewable energy sources: A review," *Renew. Sustain. Energy Rev.*, vol. 16, no. 7, pp. 4982–4993, 2012.
- [2] K. Seifi and M. Moallem, "An Adaptive PR Controller for Synchronizing," *IEEE Trans. Ind. Electron.*, vol. 66, no. 3, pp. 2034–2043, 2019.
- [3] G. Mohapatra, "Current control of a PV integrated CHB- Multilevel inverter using PR Controller," *2018 Technol. Smart-City Energy Secur. Power*, pp. 1–6, 2018.
- [4] N. S. Kumar and M. Schlenk, "Performance Analysis of PI Controller and PR Controller Based Three - Phase AC-DC Boost Converter with Space Vector PWM," vol. 118, no. 24, pp. 1–16, 2018.
- [5] S. Golestan, M. Ramezani, M. Monfared, and J. M. Guerrero, "A D-Q synchronous frame controller for single-phase inverters," *Int. Rev. Model. Simulations*, vol. 4, no. 1, pp. 42–54, 2011.
- [6] B. Bahrani, S. Member, A. Karimi, B. Rey, and A. Rufer, "Decoupled dq -Current Control of Grid-Tied Voltage Source Converters Using Nonparametric Models," *IEEE Trans. Ind. Electron.*, vol. 60, no. 4, pp. 1356–1366, 2013.
- [7] R. Teodorescu, M. Liserre, and P. Rodriguez, *Grid Converters for Photovoltaic and Wind Power Systems*. 2011.
- [8] X. S. Yang, *Studies in Computational Intelligence 516 Cuckoo Search and Firefly Algorithm*. 2013.
- [9] R. N. Mantegna, "Fast, accurate algorithm for numerical simulation of Lévy stable stochastic processes," *Phys. Rev. E*, vol. 49, no. 5, pp. 4677–4683, May 1994.